Thermodynamic approach to creep and plasticity

Ritva Löfstedt
Institute for Theoretical Physics, University of California, Santa Barbara, California 93106
(Received 26 November 1996)

A solid subjected to a small load distorts rapidly in the manner predicted by elasticity theory. On a much longer time scale, the solid will creep. This dissipative motion is an important consideration in the engineering design of, for example, aircraft engines, but the macroscopic equations of motion describing this deformation are based on empirical observations. The principles of thermodynamics specify the dissipative fluxes appropriate to the classical equations of elasticity, which include one, unique to solids, which describes creep. The thermodynamic theory is presented, and the insights into the underlying microscopic mechanisms of creep, gleaned from the macroscopic formalism, are also discussed. [S1063-651X(97)10506-2]

PACS number(s): 05.90.+m, 03.40.Dz, 81.40.Lm

How do solids differ from liquids? Distinguishing characteristics of solids include the ability to support shear forces, the appearance of long-range spatial and temporal order, and creep, the slow dissipative deformation of a solid under a small load [1–3]. Creep occurs in solids in addition to a much more rapid elastic response to a load. If the load is subsequently removed only the elastic portion of the strain relaxes. Creep thus represents an irreversible contribution to the equations of motion of a solid, not described by elasticity theory.

Andrade [4] attributed creep to ''rearrangement or rotation of small parts of a crystalline nature,'' i.e., dislocation motion, and differentiated creep mechanisms by their characteristic strain rate. In Fig. 1 is shown the length of a bar under constant load as a function of time [5]. Following an immediate elastic strain, the bar grows at a decreasing rate during primary creep. At sufficiently low temperatures such creep behavior, also termed ''logarithmic'' creep, extends indefinitely in time; the later stages of creep are suppressed. Primary creep is typically attributed to thermally activated dislocation motion [6,7]. Dislocations move as thermal fluctuations excite them over their activation barriers. Those dislocations with the smallest activation energy leave the system first, and the remaining dislocations are ever more energetically unfavorable to budge. The exhaustion of the active dislocation density leads to a decreasing strain rate.

During secondary, or steady-state, creep, dislocation mills, such as Frank-Read sources, are formed and produce new dislocations. Through variously described scenarios, the production, annihilation, and interference of dislocations yield a constant strain rate. These models include Nabarro-Herring creep [8,9] where vacancies diffuse through crystals in response to concentration gradients, and Orowan's balance of the rate of work hardening with the rate of diffusion-controlled recovery [10]. This is also the regime of ''power-law'' creep, where the strain rate is proportional to some power n (>1) of the applied stress. Such a power law is achieved in Weertman's creep model [11], where dislocation mills operate on many parallel slip planes, and the resultant dislocations interact and annihilate through dislocation climb.

As the dislocation density increases, the bar can eventually fail under the constant load, which marks the culmination of tertiary creep. During this final creep stage dislocations accumulate, cracks form and fracture brittle materials, voids coalesce, and necking ensues in ductile ones. The three stages of creep are often summarized in a law of the form [5]

$$\delta\epsilon = A\ln t + Bt^n + e^{Ct}, \tag{1}$$

where $\delta\epsilon$ is the creep strain of the solid. The freedom to choose the three coefficients and the exponent empirically implies rather a good fit to any experimental circumstance.

The empirical data on creep are most usefully summarized in deformation-mechanism maps [12], where creep mechanisms and their corresponding strain rates are plotted as functions of temperature and applied stress (Fig. 2). Such maps prove useful in the engineering design of, e.g., reactor components and aircraft engines, where creep must be reduced to strict tolerances. Parameters such as chemical composition and crystalline size can be adjusted to alter the topography of the maps and identify the materials which satisfy the tolerance limits. Thermodynamic formalisms,

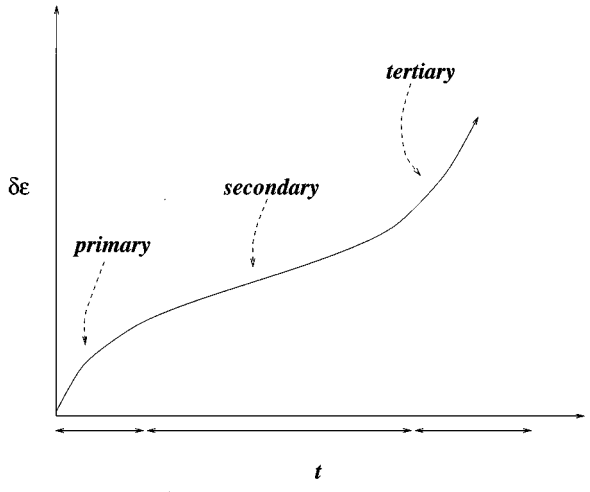

FIG. 1. The creep strain of a rod under constant load as a function of time. The behavior is typically divided into primary creep, characterized by a decreasing strain rate, secondary creep with a constant strain rate, and tertiary creep, with an increasing strain rate, culminating in failure.

 © 1997 The American Physical Society

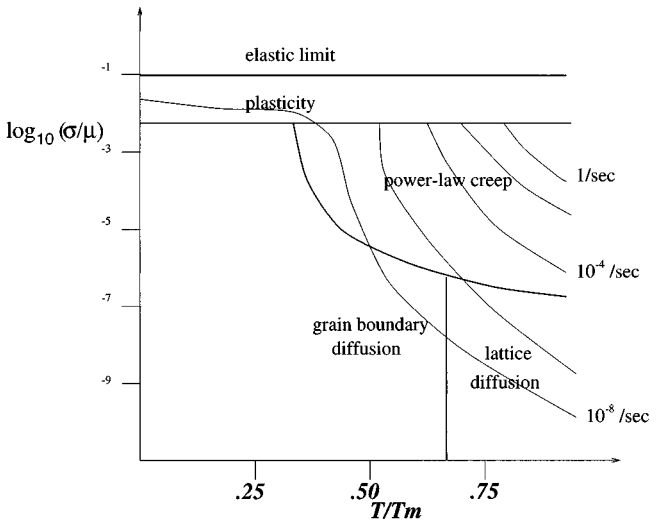

FIG. 2. A typical deformation-mechanism map, where strain rates and the deformation mechanisms are plotted as functions of temperature (normalized to the melting point) and applied stress (normalized to the shear modulus). By changing the chemical composition of a material the topography of the map can be altered and plastic deformation reduced to within tolerance limits.

such as those of Rice and Asaro and Rice [13], yield constitutive equations which successfully describe the macroscopic deformations which result from specific microstructural rearrangements, such as metallic slip and shear strain localization. Such formalisms remain empirically based, however, in the sense that the microscopic deformation mechanism which dominates the macroscopic motion must be known in order that the correct constitutive law be used.

Despite the success of such empirical approaches, a theoretical model for creep, at the level of the equations of elasticity, remains elusive. Thermal activation models must grapple with the contradiction of creep at liquid helium temperatures, where the creep curves of cadmium at 4.2 and 1.2 K differ by only 10% in their strain rates [14]. Extrapolation of the creep data from the experimental torsion, tension, and bending tests to the design of real machine components is involved; already the generalization to multiaxial stress relies on simplifying assumptions about the geometry of the yield surface [15]. Quantitative reproducibility of creep measurements is hampered by the sensitivity of creep rates to small irregularities in the experimental apparatus. For example, generalizations about the behavior of particular solids under simple tension must correct for variations in crystalline axis alignment, the presence of thermal gradients, and the precise boundary conditions imposed by the load [3].

The most pressing question posed by creep concerns the status of elasticity theory. Given that creep phenomena are long-time, long-wavelength effects, is there no macroscopic theory, at the level of hydrodynamics, which presents a unified picture of the behavior of solids? If not, it is intrinsically puzzling that decidedly macroscopic motion, such as the bending of a marble mantelpiece under its own weight [16], resists description within a thermodynamic framework. Since hydrodynamics cannot be derived from microscopic first principles, such a conclusion would imply that the macroscopic motion of solids lacks any theoretical understanding.

Eckart [17,18] developed a formal procedure by means of which he could deduce the leading-order dissipative terms appropriate to a hydrodynamic theory. Applying this procedure, which entails restricting the dissipative terms to satisfy energy conservation and entropy production, to an Eulerian fluid, yields the familiar Navier-Stokes equations characterized by shear and bulk viscosities and thermal conductivity. Eckart applied the same formalism to the equations of elasticity, and found in addition to viscosity and thermal conductivity a leading-order dissipative term unique to solids, which describes plastic deformation.

The classical equations of elasticity may be written as conservation of mass,

$$\frac{\partial \rho}{\partial t} + \vec{\nabla} \cdot \rho \vec{\nu} = 0, \tag{2}$$

conservation of momentum,

$$\frac{\partial \rho \nu_i}{\partial t} + \frac{\partial}{\partial r_j} (P \delta_{ij} + \tau_{ij} + \rho \nu_i \nu_j) = 0, \tag{3}$$

conservation of entropy,

$$\frac{\partial \rho s}{\partial t} + \vec{\nabla} \cdot \rho s \vec{\nu} = 0, \tag{4}$$

and what may be termed conservation of the lattice,

$$\frac{\partial \vec{R}}{\partial t} + (\vec{\nu} \cdot \vec{\nabla}) \vec{R} = 0, \tag{5}$$

Here $\rho(\vec{r},t)$ is the density, $\vec{\nu}(\vec{r},t)$ is the velocity, $P(\vec{r},t)$ is the hydrostatic pressure, $\tau_{ij}(\vec{r},t)$ is the shear stress tensor, $s(\vec{r},t)$ is the entropy per gram, and $\vec{R}(\vec{r},t)$ is the position at time 0 of a particle which at time t is at $\vec{r}$. The first and second laws of thermodynamics are expressed in the form

$$d\epsilon = T ds + P d\left(\frac{1}{\rho}\right) + \left(\frac{\partial \epsilon}{\partial m_{ij}}\right) dm_{ij}, \tag{6}$$

where ϵ is the internal energy of the solid per gram, T is the temperature, and m_{ij} is the strain tensor at constant density. At linear order in the strains,

$$m_{ij} = \frac{1}{2}\left(\frac{\partial R_i}{\partial r_j} + \frac{\partial R_j}{\partial r_i} - \frac{2}{3} \delta_{ij} (\vec{\nabla} \cdot \vec{R}) \right). \tag{7}$$

Using Eq. (6), and Eqs. (2)–(5), conservation of energy determines the first-order expressions for

$$P = \kappa \vec{\nabla} \cdot (\vec{R} - \vec{r}) \tag{8}$$

and

$$\tau_{ij} = \mu \left(\frac{\partial R_i}{\partial r_j} + \frac{\partial R_j}{\partial r_i} - \frac{2}{3} \delta_{ij} (\vec{\nabla} \cdot \vec{R}) \right), \tag{9}$$

where κ is the bulk modulus, and μ is the shear modulus. The presence of the shear stress tensor and the need for Eq. (5) to close the set of equations is what distinguishes these equations from the Euler equations of fluid mechanics.

To introduce dissipation into these equations Eckart [17] imposed the condition of entropy production while maintaining the conservation of energy [19,20]. The dissipative fluxes include the effects of thermal conductivity and bulk and shear viscosity, which shall henceforth be neglected. Any modification of Eqs. (2)–(5) must also be consistent with the conservation laws, Galilean covariance, and symmetry principles. To leading order, Eckart replaced Eqs. (4) and (5) by

$$\frac{\partial \rho s}{\partial t}+\vec{\nabla}\cdot\rho s\vec{\nu}=\frac{(\tau_{ij})^2}{\tau_E} \tag{10}$$

and

$$\frac{\partial}{\partial r_j}\left(\frac{\partial R_i}{\partial t}+(\vec{\nu}\cdot\vec{\nabla})R_i\right)=-\frac{\tau_{ij}}{\tau_E}, \tag{11}$$

where τ_E is a characteristic time for the elastic shear stress to relax. Eckart expressed Eq. (11) in terms of the metric $g_{ij}=(\partial R_l/\partial r_i)(\partial R_l/\partial r_j)$ of the initial (relaxed) state. He interpreted the irreversible contribution to the metric as replacing the elastic constraint of ''relaxability-in-the-large,'' where all strains are relaxed by removing external loads, by the plastic ''relaxability-in-the-small,'' where internal elastic strains may be relaxed only by cutting the material. The latter principle, Eckart showed, was sufficient to maintain a Riemannian geometry of strain.

The form of Eq. (11) closely resembles the constitutive equations describing viscoelasticity, which are frequently applied to describe slip of metallic crystals. Note, however, that Eckart's term does not allow for a characteristic ''yield stress'' to which the shear stress relaxes. Rather Eq. (11) indicates that the equations of elasticity are mathematically unstable, since the leading-order dissipation renders the solid unable to support a shear. In a real physical system, the characteristic time constants would differ on the various slip planes of an anisotropic crystal, and these time constants may be sufficiently long that relaxation effects can be ignored on the laboratory time scale.

The form of Eqs. (10) and (11) is not unique. An additional dissipative term which satisfies the constraints of energy conservation and entropy production would transform Eqs. (4) and (5) to yield

$$\frac{\partial \rho s}{\partial t}+\vec{\nabla}\cdot\rho s\vec{\nu}=d\left(\frac{\partial(\tau_{ij}r_{ik})}{\partial r_j}\right)^2, \tag{12}$$

$$\frac{\partial R_i}{\partial t}+(\vec{\nu}\cdot\vec{\nabla})R_i=d\frac{\partial(\tau_{kj}r_{ik})}{\partial r_j}, \tag{13}$$

where $r_{ij}=(\partial r_i/\partial R_j)_{R_{k\neq j}}$, and Eckart's terms have been suppressed. Equations (12) and (13) describe a ''diffusion'' of the original lattice, which is equivalent to a plastic deformation. The elastic strains are measured relative to the reference lattice $\vec{R}$. If one applies a load to a solid, according to Eq. (13), this reference lattice will on long-time scales diffuse in such a way as to reduce strain gradients. Upon removal of the load, the solid will relax the elastic part of the strains, to the new position of the reference lattice.

In what follows, I shall investigate the material behavior implied by Eqs. (12) and (13). The viscoelastic contribution, whose behavioral consequences have been explored in detail elsewhere [15] will be neglected. Equations (12) and (13) describe the lowest-order dissipative correction to a robust elastic solid state, namely, one which supports a uniform shear stress [21]. The response in Eq. (13) bears similarity to the phenomenological predictions of strain-gradient plasticity [22]. There, gradient effects are considered as an additional contribution to the equations of plastic flow. Here, qualitatively different material behavior is predicted in the regime where viscoelastic creep is suppressed, and inelastic response to shear stress gradients is the dominant mechanism of plastic flow.

Requiring that the entropy production be positive means that in Eq. (12) the diffusion coefficient $d\geqslant 0$; since a perfect lattice does not creep, we specify, $d\propto\rho_\omega$, the local density of dislocations in the solid. The presence of a higher derivative in Eq. (13) requires the application of another boundary condition. We can solve for the velocity in Eq. (13) to give

$$\nu_i=\left\{d\,\frac{\partial(\tau_{lj}r_{lk})}{\partial r_j}-\frac{\partial R_k}{\partial t}\right\}(J^{-1})_{ik}, \tag{14}$$

where

$$J=J\left(\frac{\partial R_x R_y R_z}{\partial r_x r_y r_z}\right), \tag{15}$$

the Jacobian matrix. To lowest order in the strains we can rewrite Eq. (14) as

$$\nu_i=-\frac{\partial R_i}{\partial t}+d\,\frac{\partial \tau_{ij}}{\partial r_j}. \tag{16}$$

In order that the surface of the solid be well defined, we take as the new boundary condition

$$\nu_{s\perp}=-\left(\frac{\partial R_\perp}{\partial t}\right)_{\text{surface}}=\dot{\ell}, \tag{17}$$

where $\nu_{s\perp}$ is the perpendicular component of the surface velocity and ℓ is the dimension of the solid which is creeping. By continuity, Eq. (2),

$$\nu_{s\perp}=\nu_\perp(\text{surface}), \tag{18}$$

the perpendicular component of the bulk velocity evaluated at the surface. Combining Eqs. (17) and (18) yields

$$d\left(\frac{\partial \tau_{\perp j}}{\partial r_j}\right)_{\text{surface}}=0. \tag{19}$$

The creep term is required to vanish at the surface. One way to satisfy such a boundary condition is to take $d\rightarrow 0$ at the surface, which implies that the dislocations are annihilated as they hit the surface.

The formal solution to elasticity with creep is obtained by putting Eq. (14) into Eqs. (2)–(4) to obtain a closed theory for $\vec{R}$, ρ, and s. Consider, for example, a standing bar acted on by gravity (Fig. 3). The equations of linear elasticity are solved subject to the force of gravity

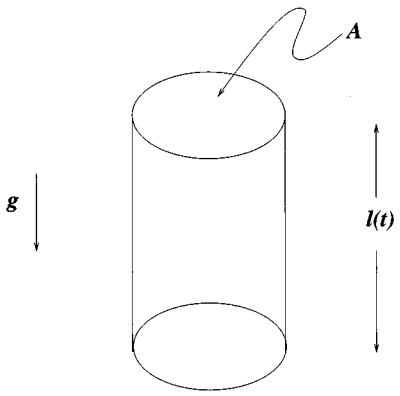

FIG. 3. A bar standing on a surface. It will creep due to the strain gradient imposed by gravity.

$$\frac{\partial(P\delta_{zi}+\tau_{zi})}{\partial r_i}=\rho g\hat{z} \tag{20}$$

and the boundary condition of vanishing shear and normal forces on the other faces yields [23]

$$\delta R_x=-\frac{\sigma\rho g}{E}(l-z)x, \quad \delta R_y=-\frac{\sigma\rho g}{E}(l-z)y,$$
$$\delta R_z=\frac{\rho g}{2E}\{l^2-(l-z)^2-\sigma(x^2+y^2)\}, \tag{21}$$

where $\delta R_i=R_i-r_i$, σ is Poisson's ratio, E is Young's modulus, and l is the length of the bar. Neglecting any changes in the radial dimension of the bar, the creep equation

$$\nu_z=-\frac{\partial R_z}{\partial t}+d\frac{\partial\tau_{zz}}{\partial z}, \tag{22}$$

with Eqs. (17) and (18) and evaluated at $z=l$ yields

$$\dot{l}=-\frac{\rho g}{E}l\dot{l}-d\frac{4}{3}\frac{\mu\rho g}{E}(1+\sigma). \tag{23}$$

The lowest-order solution

$$(l_0-l)\left(1+\frac{\rho g l_0}{2E}\right)\approx\frac{4}{3}\frac{d\mu\rho g}{E}(1+\sigma)t \tag{24}$$

gives that the length of the bar decreases linearly in time. This constant creep rate, a characteristic of secondary creep, is perhaps not surprising since we have assumed that d, and therefore the density of dislocations in the bar, is constant. Since at the boundaries the dislocations are steadily being annihilated, this constancy implies an equal rate of production of dislocations in the bulk of the bar.

The complementary scenario, viz., where the dislocation, or more generally, defect density is not replenished, requires additional information about the dynamics of the dislocation loops. Including the dependence on the additional variable $\vec{\omega}$, a local (average) Burgers vector, the equations of elasticity are revised as follows [24]. Momentum conservation (3) acquires an additional stress contribution

$$\frac{\partial\rho\nu_i}{\partial t}+\frac{\partial}{\partial r_j}(P\delta_{ij}+\tau_{ij}+\rho\nu_i\nu_j+\lambda\omega_i\omega_j)=0, \tag{25}$$

where λ is a mutual interaction energy of dislocations which enters the first law (6) as

$$\left(\frac{\partial\rho\epsilon}{\partial\omega_i}\right)_{s,p,m_{ij}}=\lambda\omega_i. \tag{26}$$

The lattice equation becomes

$$\frac{\partial R_i}{\partial t}+(\vec{\nu}\cdot\vec{\nabla})R_i=d\frac{\partial\tau_{ij}}{\partial r_j}-\gamma\{\vec{\omega}\times(\vec{\nabla}\times\lambda\vec{\omega})\}_i, \tag{27}$$

and the equation of motion for the Burgers vector is

$$\frac{\partial\vec{\omega}}{\partial t}=\vec{\nabla}\times\{(\vec{\nu}+\delta\vec{\nu})\times\vec{\omega}\}, \tag{28}$$

where

$$\delta\nu_i=\alpha\{\vec{\omega}\times(\vec{\nabla}\times\lambda\vec{\omega})\}_i+\gamma\frac{\partial\tau_{ij}}{\partial r_j}. \tag{29}$$

The dissipative terms in Eqs. (28) and (29) are again specified by requiring energy conservation and entropy production. Onsager reciprocity establishes the equivalence of the γ's and entropy production being positive also requires that $\gamma^2<\alpha d$. Since $d\propto\rho_\omega$ in the limit of dilute dislocation density, we take $\gamma\propto\rho_\omega$ to satisfy the inequality. In the same dilute limit we shall neglect terms involving mutual interactions of the Burgers vectors, and take the limiting form of Eq. (29) where the dislocation density is convected along at the creep velocity:

$$\frac{\partial\vec{\omega}}{\partial t}=\vec{\nabla}\times(\delta\vec{\nu}\times\vec{\omega}), \quad \delta\nu_i=\gamma\frac{\partial\tau_{ij}}{\partial r_j}. \tag{30}$$

Consider now the standing bar acted on by gravity, taking into account the time dependence of the dislocation density. In the dilute limit, the dislocations do not interact, and if one assumes a slowly spatially varying distribution of dislocations in the bulk, $\rho_\omega\propto|\vec{\omega}|$, and $\vec{\omega}$ can be replaced by $|\vec{\omega}|$ in Eq. (30). Assuming that the depletion of dislocations from the bulk equals the net flux of $\vec{\omega}$ through the surface,

$$\int dV\left(\frac{\partial|\vec{\omega}|}{\partial t}\right)=-\gamma\frac{4}{3}\mu\rho g|\vec{\omega}|(1+\sigma)A, \tag{31}$$

where A is the cross-sectional area of the bar, and V is its volume. Using this time dependence of the diffusion coefficient d in Eq. (23), and solving for the length of the bar, the ''exhaustion creep'' behavior is described by

$$l_0 - l \approx l_0 |\vec{\omega}_0| \left(\frac{d}{\gamma}\right) \ln\left(1 + \frac{4}{3}\frac{\mu p g}{E}(1+\sigma)\frac{\gamma}{|\vec{\omega}|} l_0 t\right), \tag{32}$$

where $\vec{\omega}_0$ is the initial value of the local Burgers vector. This result is in agreement with the logarithmic creep of the empirical relations. To describe the crossover regime from primary to secondary creep the full dependence of creep on the mutual interaction of dislocations, including the possibility of dislocation production such as a Frank-Read source, would have to be taken into account.

The richness of creep behavior is illustrated by the complexity of the two-dimensional deformation-mechanism maps [12] (Fig. 2). While various microscopic models may describe individual mechanisms at least qualitatively, transitions between mechanisms are typically only empirically observed. For example, the behavior of a sapphire fiber under a tensile load is a very strong function of its temperature [25]. At lower temperatures, hardly any creep strain is discernible before fracture. Experiments and theories have identified spherical voids which form during the fabrication of sapphire fibers as the likely culprits in the fracture. At lower temperatures these voids are unstable to surface diffusion, where the surface atoms migrate from regions of high curvature towards those of lower curvature, and deform into ellipsoids, with their major axis perpendicular to the tension. However, along with the increasing sharpness of the ellipse profile comes increased stress concentration at the tips. This ellipsoidal shape is susceptible to fracture in accordance with the Griffith criterion [26].

At higher temperatures, sapphire fibers can maintain creep strains of up to 10%. In this region of parameter space, surface diffusion is no longer a dominant deformation mechanism. Instead empirical creep equations predict that the spherical voids distort into ellipsoids elongated in the direction parallel to the tension. These are shapes of diminishing stress intensities, and they are stable against crack formation. Despite its dramatic consequences, the behavioral transition in sapphire as a function of temperature is unexplained.

Clearly a macroscopic theory cannot reveal an underlying microscopic mechanism for creep. However, the macroscopic behavior which follows must be describable by the thermodynamic formalism; in this case, the two behaviors are obtained by solving the dissipative elastic equations subject to two different boundary conditions. As of yet we have satisfied the boundary condition on the creep term (19) by taking $d \to 0$ at the surface. However, if the dislocations do not annihilate as they hit the surface, the diffusion constant does not vanish. In addition, the presence of dislocations implies a stress discontinuity at the boundary. Condition (19) can still be satisfied, however, by taking

$$\left(\frac{\partial \tau_{\perp j}}{\partial r_j}\right)_{\text{surface}} = 0 \tag{33}$$

as the boundary condition subject to which the elastic equations should be solved.

Consider a circular hole in a two-dimensional plate, with a tensile force S acting on it at infinity. The general solution to the elastic equations in this (dipolar) geometry is given by [27]

$$\begin{aligned} P + \tau_{rr} &= A + \frac{B}{r^2} - \cos 2\theta \left(2A' + \frac{6C'}{r^4} + \frac{4D'}{r^2}\right), \\ P + \tau_{\theta\theta} &= A - \frac{B}{r^2} + \cos 2\theta \left(2A' + 12B' r^2 + \frac{6C'}{r^4}\right), \\ \tau_{r\theta} &= \sin 2\theta \left(2A' + 6B' r^2 - \frac{6C'}{r^4} - \frac{2D'}{r^2}\right), \end{aligned} \tag{34}$$

where the coefficients are specified by the boundary conditions. Using these solutions in Eq. (16) gives for the lowest-order, angle-dependent creep rates

$$\begin{aligned} \nu_r &= -\frac{\mu d}{E}\cos 2\theta \left\{16B' r(-2\sigma - 1) + \frac{16D'(-1-2\sigma)}{3r^3}\right\}, \\ \nu_\theta &= -\frac{\mu d}{E}\sin 2\theta \left\{16B' r(2\sigma + 1) + \frac{16D'(1+2\sigma)}{3r^3}\right\}. \end{aligned} \tag{35}$$

If the dislocations in the bulk are annihilated as they hit the surface, then we use the solution to linear elasticity, Eq. (34), satisfying the boundary conditions

$$(P + \tau_{rr})_{r=0} = 0 \tag{36}$$

and

$$\tau_{r\theta}(r = a) = 0, \tag{37}$$

where a is the radius of the circular hole. This solution

$$\begin{aligned} A &= \frac{S}{2}, \quad B = -\frac{Sa^2}{2}, \quad A' = -\frac{S}{4}, \quad B' = 0, \\ C' &= -\frac{Sa^4}{4}, \quad D' = \frac{Sa^2}{2} \end{aligned} \tag{38}$$

is then used in Eq. (35) to solve for the creep behavior. This is illustrated in Fig. 4(b), and the creep is seen to elongate the circle in the stable direction.

If the dislocations build up at the surface, we can calculate the effect of the creep term when the dislocation density at the surface has reached a steady-state value. In this case, the equations of linear elasticity should be solved subject to the boundary conditions

$$\left(\frac{\partial \tau_{rj}}{\partial r_j}\right)_{r=a} = 0 \tag{39}$$

and

$$\tau_{r\theta}(r = a) = 0, \tag{40}$$

whose solution is

$$\begin{aligned} A &= \frac{S}{2}, \quad B = -\frac{Sa^2}{2}, \quad A' = -\frac{S}{4}, \quad B' = 0, \\ C' &= -\frac{Sa^4}{12}, \quad D' = 0. \end{aligned} \tag{41}$$

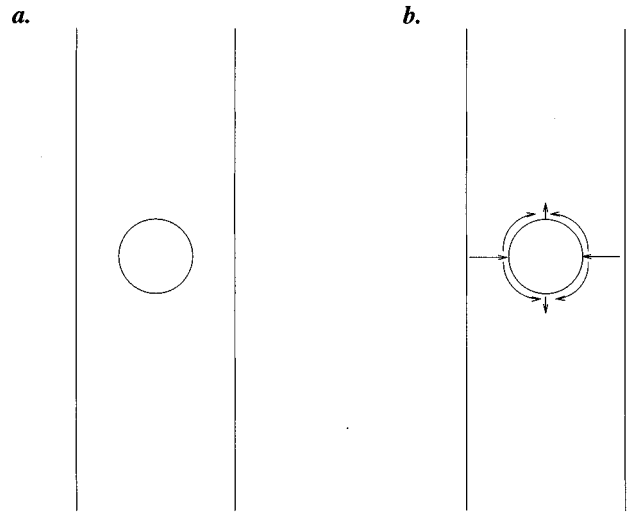

FIG. 4. The distortion of spherical voids in sapphire fibers under tension. (a) The solution to the creep equation (33) if dislocations pile up at the surface. Both radial and angular creep are suppressed, and the material is susceptible to other means of fracture. Such behavior is observed at lower temperatures. (b) The solution to Eq. (33) if dislocations annihilate at the surface. The sphere elongates in the direction of the tension, and the stresses are diminished. Such (stable) strain is observed at higher temperatures.

Again, the resultant creep of the circular shape can be found by using Eq. (41) in the creep equations (35) and is found to vanish identically. The circular shape in this instance resists elongation in the direction of the external tension and the accompanying diminution of the geometrical stress concentration. Thus, with this boundary condition, the elastic solution is instead susceptible to other deformation mechanisms, such as surface diffusion, which work to distort the ''hardened'' surface into the unstable cracklike shape. The macroscopic theory thus indicates that the transition in deformation mechanism as a function of temperature is related to the ability of dislocations to pass through the surface; at high temperatures the dislocations can get through, while at low temperatures they build up at the surface. Thus the nature of the macroscopic theory may give insight into the workings on a microscopic scale.

The theory considered herein is clearly in a rudimentary form. To connect to current empirical creep equations the full dependence of the elastic constants on the crystalline geometry should be taken into account [28]. Rather than assuming the ''amorphous'' elasticity expressed by one bulk and one shear modulus, one could systematically incorporate the preferred slip planes and reproduce the sensitivity of creep to alignment. Given the high-temperature apparatus used in most creep tests, the full set of thermodynamic dissipative fluxes, notably thermal conductivity and viscoelastic relaxation, Eq. (13), ought to be included in the analysis of a laboratory experiment. Finally, rather than taking steady-state solutions to the weakly dissipative equations, the dynamics of dislocations as given by Eqs. (25)–(29) contains both transient behavior and nonlinear interactions. The full equations might allow for a thermodynamic description of plasticity [29] and lend some insight into the accompanying effects of hysteresis and acoustic emission [30].

The analysis in this paper is motivated by the presently frustrating state of fracture theory. The classic crack description due to Inglis solves the elastic equations around an elliptical hole in a stressed plate [31]. The limit of an infinitesimally wide ellipse, which is the basis of current descriptions of fracture, is riddled with singularities and resultant dynamic instabilities [32]. Inclusion of an inelastic dissipation might allow for a self-consistent calculation of a dynamic crack profile. The competing time scales governing elastic crack propagation and the dissipative forces would determine whether the dynamic solution results in fracture or plastic deformation. Perhaps through such an analysis one could even define the engineering concepts of ''brittleness'' and ''ductility'' more rigorously, as thermodynamic equations of state.

I am grateful for the comments and criticisms of J. Langer, G. Mazenko, S. Putterman, and Z. Suo. This work was supported by the ITP's NSF Grant No. 94-07194.

[1] F. Garofolo, *Fundamentals of Creep and Creep-Rupture in Metals* (MacMillan, New York, 1965).
[2] J.-P. Poirier, *Creep of Crystals* (Cambridge, Cambridge, England, 1985).
[3] R. W. Evans and B. Wilshire, *Creep of Metals and Alloys* (Institute of Metals, London, 1985).
[4] E. N. da C. Andrade, Proc. R. Soc. London, Ser. A **84**, 1 (1910).
[5] R. W. K. Honeycombe, *The Plastic Deformation of Metals*, 2nd ed. (Arnold, London, 1984), Chap. 13.
[6] G. I. Taylor, Proc R. Soc. London, Ser. A **145**, 362 (1934).
[7] N. F. Mott and F. R. N. Nabarro, *Report on Conference on Strength of Solids* (Physical Society, London, 1948), p. 1.
[8] F. R. N. Nabarro, *Report on Conference on Strength of Solids* (Physical Society, London, 1948), p. 75.
[9] C. Herring, J. Appl. Phys. **21**, 437 (1950).
[10] E. Orowan, Proc. Phys. Soc. London **52**, 8 (1940).
[11] J. Weertman, J. Appl. Phys. **28**, 1185 (1957).
[12] H. J. Frost and M. F. Ashby, *Deformation-Mechanism Maps* (Pergamon, New York, 1982), especially Chap. 19.
[13] J. R. Rice, J. Mech. Phys. Solids **19**, 433 (1971); R. J. Asaro and J. R. Rice, *ibid.* **25**, 109 (1977).
[14] W. Meissner, M. Polanyi, and E. Schmid, Z. Phys. **66**, 477 (1930).
[15] W. N. Findley, J. S. Lai, and K. Onaran, *Creep and Relaxation of Nonlinear Viscoelastic Materials* (Dover, New York, 1976).
[16] Lord Rayleigh, Proc. R. Soc. London, Ser. A **144**, 266 (1934).
[17] C. Eckart, Phys. Rev. **58**, 267 (1940).
[18] C. Eckart, Phys. Rev. **73**, 373 (1948).
[19] R. L. Seliger and G. B. Whitham, Proc. R. Soc. London, Ser. A **305**, 1 (1968).
[20] S. J. Putterman, *Superfluid Hydrodynamics* (North-Holland, Amsterdam 1974).

[21] P. D. Fleming and C. Cohen, Phys. Rev. B **13**, 500 (1976).

[22] N. A. Fleck and J. W. Hutchinson, J. Mech. Phys. Solids **41**, 1825 (1993); N. A. Fleck, G. M. Muller, M. F. Ashby, and J. W. Hutchinson, Acta Metall. Mater. **42**, 475 (1994).

[23] L. D. Landau and E. M. Lifshitz, *Theory of Elasticity*, 3rd ed. (Pergamon, New York, 1986).

[24] I. M. Khalatnikov, *An Introduction to the Theory of Superfluidity* (Addison-Wesley, New York, 1989), Chap. 13. The inclusion of rotational motion in the two-fluid theory of helium is analogous. Note that his definition of the interaction differs slightly from mine; he uses $(\partial\epsilon/\partial\vec{\omega})_{p,s,m_{ij}}=\lambda\vec{\omega}$ in place of Eq. (24).

[25] D. J. Gooch and G. W. Groves, J. Mater. Sci. **8**, 1238 (1973); R. F. Firestone and A. H. Heuer, J. Am. Ceram. Soc. **59**, 24 (1976); B. Sun, Z. Suo, and A. G. Evans, J. Mech. Phys. Solids **42**, 1653 (1994).

[26] A. A. Griffith, Philos. Trans. R. Soc. London, Ser. A **221**, 163 (1921).

[27] S. P. Timoshenko and J. N. Goodier, *Theory of Elasticity* (McGraw-Hill, New York, 1970), p. 35.

[28] F. R. N. Nabarro, *Theory of Crystal Dislocations* (Dover, New York, 1967).

[29] C. R. Calladine, *Theory of Plasticity* (Holsted, New York, 1985).

[30] T. Erber, S. A. Guralnick, and S. C. Michels, Ann. Phys. (N.Y.) **224**, 157 (1993).

[31] C. E. Inglis, Trans. Inst. Nav. Arch. **55**, 219 (1913).

[32] E. H. Yoffe, Philos. Mag. **42**, 739 (1951); E. S. C. Ching, J. S. Langer, and H. Nakanishi, Phys. Rev. Lett. **76**, 1087 (1996).